MAGNETIC NANOPARTICLE FORMULATIONS AS MRI CONTRAST AGENTS: A REVIEW

Abstract

Magnetic nanoparticles have been developed for use in a number of interesting biological applications, including contrast agents in magnetic resonance imaging (MRI), drug delivery vectors, and mediators for converting electromagnetic energy to heat. Massive attempts have been made to create magnetic nanoparticles for MRI contrast agents. Herein, we show the synthesis methods for perpetration of iron oxide nanoparticles with surface modifications and also include characterization techniques used for size, surface and magnetic properties detection. A brief discussion on magnetic nanoparticles, toxicity and angiogenesis activity is included. In this review, we discuss to develop iron oxide based nanoparticles (NPs) formulations, preferably aqueous dispersions which are superparamagnetic, stable and biocompatible with suitable cell lines, for application as T_2 MRI contrast agents with better r_2 relaxivity.

Keywords: Magnetic nanoparticles, magnetic resonance imaging (MRI), nanoparticles (NPs).

Authors

Dr. Nooris Momin
Research Associate
Physics
Department of Physics, University of Mumbai, Vidyanagari, Santacruz (E), Mumbai
Flat no. 32, B wing, 3rd floor, St. Andrew's Apartment, Meghraj Sethi Marg, Morland Road, Agripada, Mumbai.
noorismomin@gmail.com

I. INTRODUCTION

Nanoparticles (NPs) exhibit heightened reactivity compared to bulk materials, thanks to their elevated surface-to-volume ratio. Among NPs, magnetic nanoparticles (MNPs) belong to a class that can be influenced by weak magnetic fields. The quest for producing uniformly sized MNPs has been a subject of intense research, owing to their wide-ranging applications encompassing magnetic data storage, ferrofluids, magnetic resonance imaging (MRI), magnetically guided drug delivery, and catalysts for carbon nanotube growth [1-3]. Investigations into MNPs are driven not only by fundamental scientific curiosity but also by their intriguing potential applications, stemming from their distinctive physical and chemical properties [4]. Superparamagnetic iron oxide nanoparticles (SPIONs) hold immense promise in biomedical domains, such as cellular therapy, tissue mending, drug transport, MRI, hyperthermia, and more [5-7]. This promise arises from their perceived lower toxicity compared to metallic counterparts. To fulfill the stringent requirements of applications like these, NPs must possess a combination of attributes: high magnetic saturation, size below 50 nm, biocompatibility, neutrality at physiological pH, chemical stability, and resistance to agglomeration. A notable challenge with NPs is their tendency to agglomerate rapidly. To mitigate this issue, various polymers, such as dextran, chitosan, polyethylene glycol (PEG), and polyvinyl alcohol, are used to coat the NPs [8-11]. Recently, iron oxide NPs with diverse coatings have garnered considerable attention due to their favorable magnetic properties in the realms of biomedicine and bioengineering. Moreover, these materials should exhibit low toxicity and high biocompatibility, as the safety of NPs in the context of human health is a critical factor for their successful medical application. Recent studies have demonstrated that thiol-containing hydrophilic ligand-coated iron oxide NPs are non-toxic to human lymphocytes, making them suitable for treating tumor cells [12]. Additionally, Fe3O4 NPs coated with chitosan display biocompatibility with human osteoblast cells [13], and sodium oleate-coated Fe3O4 NPs do not exert any toxic effects on 3T3 cells [14]. The presence of surface coatings has been shown to enhance aqueous dispersion stability, reduce agglomeration, and ensure excellent biocompatibility, rendering them promising candidates for various biomedical applications.
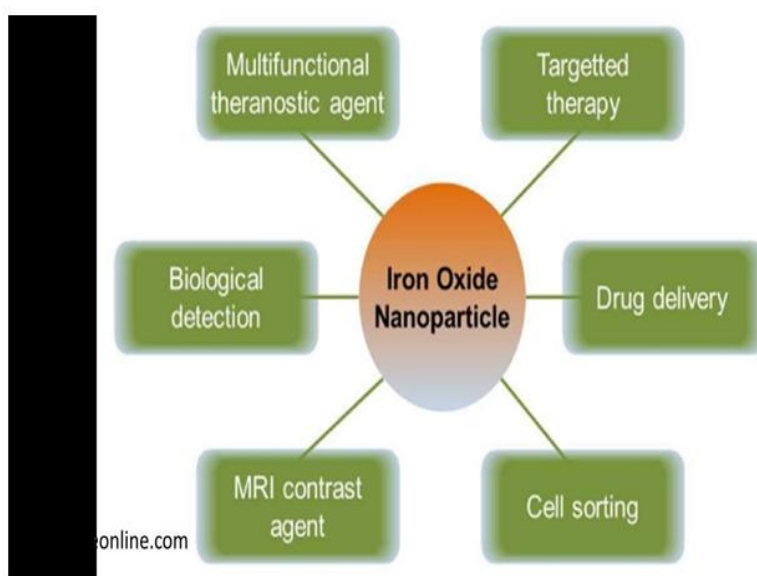
Figure 1: Applications of Magnetic Nanoparticles.

II. MAGNETISM IN ULTRAFINE PARTICLES

Nanoscale magnetism in materials is quite fascinating. In general, nanoparticles' characteristics are very different from those of their bulk counterparts.

1. **Single Domain Particle:** There may be a minimum domain size in a big body below which the benefits of lowering magnetostatic energy outweigh the energy cost of domain development. This suggests that there would be no domain separation for a single particle with a size similar to the minimum domain size.

   Qualitatively, it is seen that a domain wall cannot fit inside a particle smaller than roughly 100 nm, leading to single domain particles. A multidomain particle has a higher domain wall energy but a lower magnetostatic energy than a single domain particle, which has a high magnetostatic energy but no domain wall energy. The form and magnetocrystalline anisotropies of a single domain particle dictate its easy direction of magnetization prior to the application of an external field. The particle cannot react through the hard direction to the new easy direction when an external field is introduced in the opposite direction [16–19].
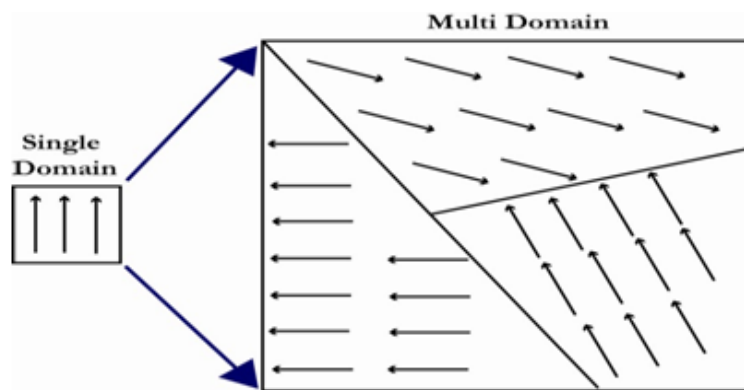
Figure 2: The effect of increasing particle size, by going from a small single domain particle to the large particle results in multi domain materials with domain boundaries.

2. **Superparamagnetism:** Below what is referred to as the blocking temperature, very small ferromagnetic or antiferromagnetic particles can exhibit characteristics similar to a large magnetic moment (or macro-spin). Upon applying a magnetic field, the condition resembles the classical limit of infinite spins, and the resulting magnetization will obey a H/T law provided by the Langevin function.

   It is important to note that the blocking temperature is affected by both the measurement time scale and the particle volume. This is because the particle undergoes a relaxation phenomenon when it moves from a blocked state, where its magnetic moment is rigidly directed in a specific direction, to a superparamagnetic state. Thus, when the magnetization of tiny particles is measured using the classical extraction technique at ambient temperature (the experiment taking about a second to complete), it can appear that the particles are superparamagnetic, while a neutron

They will appear "blocked" in a diffraction experiment because of the brief neutron-spin contact period [15].

In 1949, L. Neel introduced the theory of superparamagnetism (although he did not explicitly use the term "superparamagnetism") for fine ferromagnetic particles [20]. He later expanded this theory to encompass fine antiferromagnetic particles in 1961 [21]. Both of these seminal articles are included in his compiled scientific works [22].
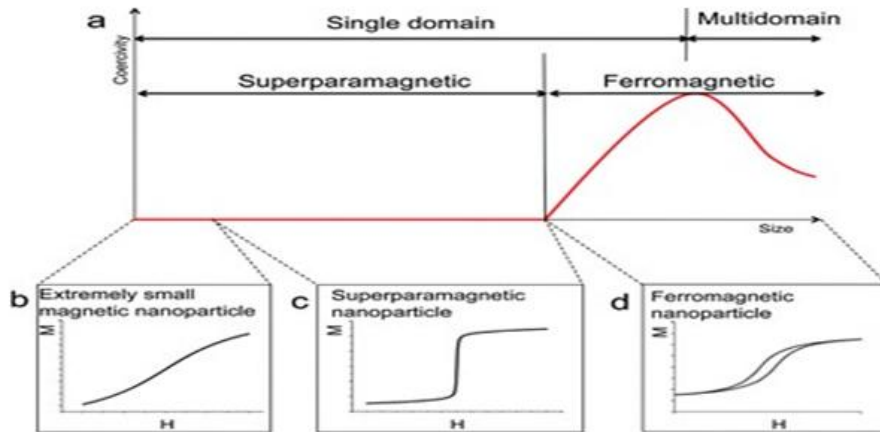
Figure 3: Size dependent variation of Hysteresis magnetization of fine particles.
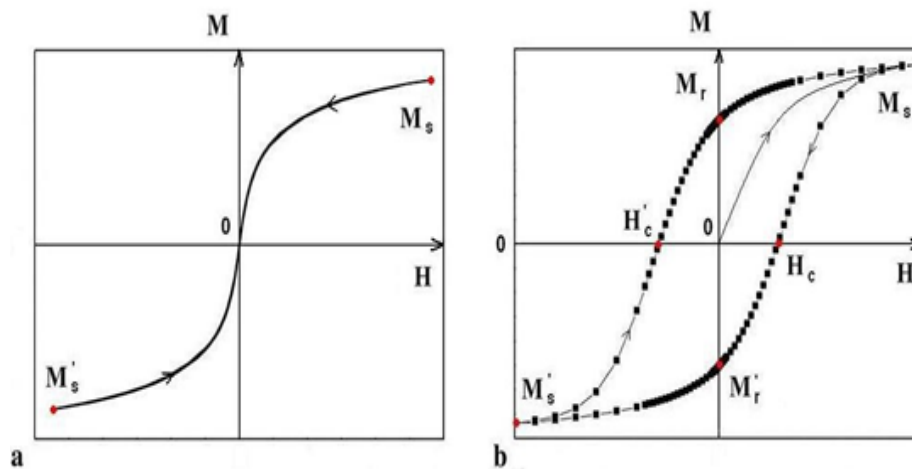
Figure 4: Comparing magnetization curves of (a) superparamagnetic and (b) ferromagnetic materials.

III. SYNTHESIS TECHNIQUES

Because even minute amounts of non-magnetic impurities can significantly change a material's characteristics, nanomagnetic materials are extremely sensitive to processing parameters and impurity levels. Therefore, selecting the right technique for creating metallic nanoparticles and their composites is essential. For example iron oxide NPs prone to oxidation even at room temperature in open atmosphere. A special care is needed for the synthesis of metallic NPs. Moreover, it is too difficult to prepare a nanocomposite comprising

a metal and an oxide. The development of a high purity material is very crucial for investigation of involved physical properties. Iron oxide nanoparticles (NPs) can be produced using a variety of techniques, including sol gel, thermal breakdown, water-in-oil emulsion, polyol, gas deposition, co-precipitation, hydothermal, and others. Each method has its own unique conditions and performance protocol, and naturally, there are NPs with various characteristics (such as shape, size distribution, average size, crystallinity, magnetic NPs, and dispersibility). There are two methods for creating nanomaterials through synthesis. The two approaches are top-down and bottom-up. The bottom-up approach method is mostly used to produce magnetic nanoparticles. Two approaches with good product quality to synthesis difficulty ratios will be compared in this paper. Co-precipitation and heat degradation are these pathways. Iron oxide nanoparticles are coated via sonication, heating, and stirring.

1. **Co-Precipitation Method:** In the field of chemistry, co-precipitation refers to the process of achieving the precipitation of substances that are typically soluble under the given conditions [23]. Co-precipitation operates through three primary mechanisms: inclusion, occlusion, and adsorption [24]. Inclusion takes place when an impurity occupies a lattice site within the crystal structure of the host material, resulting in a crystallographic defect. This occurs when the ionic radius and charge of the impurity closely resemble those of the host material. An adsorbate is an impurity that is weakly bound or adsorbed onto the surface of the precipitate. On the other hand, occlusion arises when an adsorbed impurity becomes physically trapped inside the growing crystal structure. Co-precipitation serves as a valuable method for synthesizing magnetic nanoparticles (NPs) [25]. It is a straightforward and convenient approach for producing iron oxides (either Fe_3O_4 or γ-Fe_2O_3) from aqueous Fe^{2+}/Fe^{3+} salt solutions by adding a base under an inert atmosphere, either at room temperature or elevated temperatures. The size, shape, and composition of magnetic nanoparticles (NPs) are contingent upon several factors, including the choice of salts (e.g., chlorides, sulphates, nitrates), the Fe^{2+}/Fe^{3+} ratio, reaction temperature, pH value, and ionic strength of the medium [25]. In recent times, the co-precipitation method has found extensive use in the controlled production of ferrite NPs with specific sizes and magnetic properties [26-29]. The co-precipitation reaction involves the simultaneous occurrence of nucleation, growth, coarsening, and/or agglomeration processes. Co-precipitation reactions exhibit the following characteristics: (i) they yield products that are generally insoluble species formed under conditions of high supersaturation; (ii) nucleation plays a pivotal role, resulting in the formation of numerous small particles; (iii) secondary processes like Oswald ripening and aggregation significantly influence the size, morphology, and properties of the final products; (iv) the supersaturation conditions necessary for precipitation are typically the outcome of a chemical reaction.

    X Ay+ (aq.) + Y Bx- (aq.) ↔ AxBy (S);
    where X = molar concentration of A, Y = molar concentration of B, y+ = ionic state of A, x- = ionic state of B

    The initial precursors' molarity and the precipitation medium's pH have a significant impact on the co-precipitated material's particle size. Controlling the size is therefore simple to accomplish. The concentration of the reactants, temperature, pH, reagent addition sequence, and mixing all have an impact on the reaction and transport rates. Impurities and reaction rates can affect the particles' structure and crystallinity.

Particle morphology is determined by various parameters, including growth rates, nucleation, and supersaturation. The crystal structure and surface energies determine the morphology of the small, compact, and well-formed particles at low supersaturation. Large, dendritic particles emerge at high super saturation levels. Compared to other preparative techniques, the co-precipitation approach has several advantages, including fast and quick preparation, easy control over particle size and composition, and numerous options for altering the particle surface state and overall homogeneity. Co-precipitation is a facile and convenient way to prepare colloidal magnetic NPs [25], and the reactions scale well to produce high amount of particles: ~10 g with yields around 85% [30-33]. In the present investigation, NPs of iron oxide were synthesized by a wet chemical route using iron chloride as a precursor. Ammonia solution and sodium hydroxide was used as the reducing agent. The reaction was done at room temperature. Similarly, for synthesis of coated NPs, the required coating agents like curcumin, dextran, PEG- 6000 were added after the precipitate formation using ammonia solution as reducing agent.

2. **Thermal Decomposition Method:** The method of synthesizing iron oxide-based nanoparticles through the thermal decomposition of organometallic precursors has been widely employed. Organic iron compounds such as Ferric acetylacetonate [Fe(acac)3], iron oleate [Fe(oleate)3], and iron pentacarbonyl [Fe(CO)5] are subjected to high-temperature decomposition within a non-polar boiling solvent, along with the presence of a capping agent [34]. However, it's worth noting that most of the precursors used in this method are toxic and environmentally unfriendly. This synthesis approach, although capable of yielding high-quality, monodisperse iron oxide nanoparticles, typically necessitates higher temperatures and involves a more intricate operation. limited distribution of sizes This route's characteristics include good crystallinity and form control [35]. With a steady heating rate, the precursor is heated to the boiling point of the solvent and maintained there for the required amount of time. Because the nucleation and growth mechanisms during breakdown can be easily distinguished and occur at distinct temperatures, a narrow size distribution is the result. It begins to nucleate at about 200–230 degrees Celsius, and it grows between 260 and 290 degrees Celsius. The NPs are covered with a capping ligand (fatty acids, hexadecylamine), which serves as a colloidal stabilizer in addition to a tool for size control [36]. These methods produce hydrophobic (not soluble in water) nanoparticles (NPs), which can be kept in non-polar solvents such as toluene, cyclohexane, and hexane. The size and form of NPs can be controlled in a number of ways. Three parameters can be adjusted to control the size: (i) the decomposition reaction temperature (which is dependent on the boiling solvent); (ii) the ratio of precursor to capping agent; and (iii) the reaction duration beyond the boiling point. The volumetric ratio of the precursor to the boiling solvent and the heating rate have the greatest effects on the NPs' morphology. Variations in the boiling solvent (di-n-hexyl ether) with a boiling point of 228 °C, hexadecene (bp 274 °C), dioctyl ether (bp 294 °C), and octadecene (bp 317 °C) were examined, as well as the amount of oleic acid capping agent used [37]. This process produces very few NPs in a single batch, but they are of excellent quality. Maintaining a steady heating rate is one of the biggest challenges of this approach, particularly in the range where nucleation and growth take place. Ferric chloride and sodium citrate are two examples of non-toxic, environmentally acceptable precursors that are preferred for "green" synthesis [38]. High-quality, non-toxic, and highly dispersible nanoparticles are produced by this process, and each batch yields a sizable amount.

IV. SONICATION

The study of sonication revolves around examining the impact of high-frequency sonic waves and their wave properties on chemical systems. Since acoustic waves possess distinct physical characteristics, they give rise to unique atomic and molecular chemistry. Sonication primarily investigates chemical reactions driven by high-frequency sound waves. When ultrasonic waves pass through a liquid, they generate small bubbles that rapidly collapse. This phenomenon is known as "cavitation" [39-41], where tiny cavities (approximately 100 microns) implode, producing significant heat, pressure, shock waves, and particle acceleration.

To achieve this, an ultrasonic power supply converts line voltage into high-frequency electric energy, typically around 20 kHz. This electrical energy is then transmitted to a probe, where it is transformed into mechanical energy. The probe, usually equipped with a titanium tip, vibrates longitudinally and transfers this motion to the titanium tip immersed in the solution. This process can lead to the formation of microscopic vapor bubbles, which experience cavitation. Once formed, these bubbles contain vapor and gas. In sonication, bubbles are typically driven below their natural frequency at high-pressure amplitudes, causing them to undergo slow expansion followed by rapid, violent collapse. During this collapse, the gas inside the bubble reaches temperatures estimated to be around 5000-8000 Kelvin and pressures exceeding 10,000 atmospheres on a nanosecond time scale.

Sonochemistry, a form of heterogeneous chemistry, occurs in systems involving liquid-liquid or solid-liquid interactions [42-44]. In practice, sonication, defined here as the irradiation of materials with high-intensity ultrasound, is employed to achieve homogeneous mixing and modify the surfaces of powders composed of different constituents. An ultrasound sonicator was utilized in this study to prepare coated iron oxide nanoparticles.

Characterization: The post-synthesis characterization techniques employed for the magnetic nanoparticles (MNPs) are as follows:

- Transmission and Scanning Electron Microscopy (TEM and SEM), both equipped with an energy-dispersive X-ray spectrometer (EDS), will be utilized to analyze surface morphology and the thickness of the coating layer. Additionally, images from Bright-field TEM (BFTEM), high-resolution TEM (HR-TEM), Fast Fourier Transform (FFT) analysis, and selected area electron diffraction (SAED) patterns will be recorded. These imaging and analysis methods will provide detailed information about the morphological, structural, and compositional aspects of the superparamagnetic iron oxide nanoparticles (SPIONs), which may vary in shape, size, and coatings.

- The structural characterization of SPIONs will be conducted using X-ray diffraction (XRD) in Bragg-Brentano (Ɵ-2Ɵ) configuration, allowing for the determination of the crystalline structure.

- Fourier Transform Infrared Spectroscopy (FT-IR) and Raman spectroscopy will be employed to identify any chemical species present in the SPIONs.

- Dynamic Light Scattering (DLS) and Zeta potential measurements will be carried out to assess the hydrodynamic size and stability of the SPIONs.

- Magnetic measurements, including saturation magnetization, coercivity, blocking temperature, and susceptibility, will be performed using a Quantum Design PPMS with a 9T VSM to determine the magnetic properties of the SPIONS.

1. **Magnetic Nanoparticles in Various Biomedical Studies:** Nanotechnology is a potential growing field as with Nanotechnology is a potential growing field as with immense application in the field of biomedicine. By 2020, 58,000 tons of NPs are expected to be generated, up from the current predicted 300 tons [45]. The combination of biomedical advancements and nanotechnology holds the potential to create a new instrument for biomedical analysis [46]. Specifically, biomedicine—which refers to the diagnosis, treatment, and cure of illnesses at the molecular level—may be associated with nanotechnology. The use of NPs (100nm and smaller) for delivery and diagnostics agents is at the forefront of projects in cancer treatment [47]. In vitro studies are becoming essential to substantiate effect of NPs on biological systems. The important property of the magnetic NPs that need to be address is that of biocompatibility with cell lines i.e. to investigate cytotoxicity.

2. **Cytotoxicity:** Ferrite or iron oxide NPs are the most widely used electromagnetic materials, finding applications over a wide range due to their low cost and high performances [48]. Alternating magnetic field heats up the ferrite NPs, allowing its applications in imaging and therapy [45]. In the recent years the research has focused on evaluating cytotoxicity of ferrite/iron oxide NPs. It is found a cell- specific response to bare iron oxide nanoparticle exposure on cell lines [49]. 3T3 cells maintained their proliferative behavior even with the addition of up to 30 ppm of iron oxide. In contrast, human mesothelioma cells displayed a significant reduction in cell viability when exposed to just 3.75 ppm of iron oxide. In a study involving COS-7 cell lines, higher concentrations of nanoparticles (ranging from 0.09 to 23.05 mM) showed no significant differences in cell behavior compared to the control group.

   Another investigation assessed the impact of bare iron oxide particles at concentrations ranging from 0 to 250 μg/ml on Rat Liver cells (BRL3A) and observed a 30% decrease in cell viability. When human fibroblast cells were exposed to PEG-coated nanoparticles, they exhibited more than 99% viability compared to the control group. However, bare iron oxide nanoparticles caused a 25–50% reduction in fibroblast viability at a concentration of 250 mg per ml.

   Furthermore, the cytotoxicity of iron oxide nanoparticles with three different surface coatings was studied. MPEG–Asp3-NH2-coated iron oxide nanoparticles showed almost no cytotoxicity at the tested concentrations. In contrast, MPEG–PAA- and PAA-coated iron oxide nanoparticles significantly reduced cell viability, with only 16% of cells remaining viable at an iron concentration of 400 mg per ml. Additionally, uncoated iron oxide nanoparticles, which adhered to the cell surface, also had a significant negative impact on cell viability as evidenced by cell counts after incubation.. This study was conducted on the OCTY mouse cell lines. In most of the studies the cytotoxicity was evaluated by viability and 3-(4,5-dimethyl-2-thiazolyl)-2,5-diphenyl-2H-tetrazolium bromide (MTT) assay. The studied interaction of magnetic microspheres with cells

(adherent human prostate cells (DU- 145) and Murine suspension lymphoma cells (EL-4), using an in vitro 3-[4,5- dimethylthiazol-2yl]-2,5- diphenyltetrazolium bromide (MTT) assay [54]. Viability and metabolic activity were reduced in all examples. However, the MTT assay is not recommended for all cell lines due to high variability and non-specificity. So our preliminary test was on human lymphocyte cells to evaluate biocompatibility for getting optimum effect for drug delivery system. The cytotoxicity effects of iron oxide coated with thiol containing hydrophilic ligands has found to be non-toxic in human lymphocytes and nitric oxide releasing iron oxide NPs are found to be toxic in human lymphocytes [12], CoFe2O4 NPs found to be biocompatible with human lymphocyte cells [55]. In the present investigation, the synthesized uncoated and coated iron oxide based NPs biocompatible studies are evaluated on human lymphocyte cells by Trypan blue dye exclusion test. There is a growing body of published research on the NPs' in-vitro cytotoxicity utilizing various cell lines. But given the vast range of NPs concentrations and exposure times included in these investigations, it is challenging to assess whether the cytotoxicity seen is physiologically meaningful. The disparity in the results obtained by the various assays could be because of the culture condition, incubation time, concentration of the NPs and the assays used for testing viability. The cytotoxicity pattern varies from one cell types to the other. The uptake of NPs into the organism often induces or suppresses some biological processes or activities. In our work we have investigated the effect of various magnetic NPs on the angiogenesis activity that is discussed below.The analysis of cytotoxicity was done using the proportion of dead cells.

The following formula was used to determine the vitality of the cells:

$$\% \text{ cell viability} = \frac{\text{No.of viable cells}}{\text{Total no.of cells}} \text{ X } 100$$

3. **Angiogenesis Activity:** The physiological process known as angiogenesis is responsible for the creation of new blood vessels from pre-existing ones. This is not the same as vasculogenesis, a biological process that creates new blood vessels from mesoderm cell progenitors and endothelium cells [56]. The regulation of angiogenesis relies on chemical signals within the body, which can trigger the repair of injured blood vessels and the creation of fresh ones. Conversely, certain chemical signals, known as angiogenesis inhibitors, disrupt the process of blood vessel formation. Typically, there is a delicate equilibrium between the stimulatory and inhibitory actions of these chemical signals, ensuring that blood vessels are generated precisely when and where they are required [57]. Angiogenesis serves as a crucial factor in diverse physiological and pathological scenarios, encompassing embryonic development, wound healing, inflammation, and tumor progression [58]. Normal growth and wound healing processes depend on angiogenesis. Angiogenesis is hampered by an imbalance of the growth factors involved in this process, which is linked to a number of illnesses, including diabetes mellitus, cancer, ophthalmic, and inflammatory conditions. Defective angiogenesis is the cause of delayed wound healing in diabetes mellitus. There are many models to study the angiogenesis activity such as mouse model and Chick Chorioallantoic membrane model. Chick Chorioallantoic membranes (CAM) derived from developing chick eggs are commonly employed in biological and biomedical research. They are utilized for exploring angiogenesis, tumor development, and investigating viruses or helminths [59-65]. The CAM model is favored due to its extensive vascularization, cost-effectiveness,

ease of access, reliability, and reproducibility. It has been extensively utilized to examine both the morphological and functional aspects of the angiogenesis process in vivo and to assess the effectiveness and mechanisms of action of proangiogenic and antiangiogenic natural and synthetic compounds [66, 68]. More recently, it has been observed that dextran hydrogel scaffolds enhance angiogenic responses and facilitate complete skin regeneration during the healing of burn wounds. [65], Using fluorescein isothiocyanate (FITC)-dextran, angiogenesis activity in mice is boosted. Biogenic silver nanoparticles made from saliva exhibit anti-angiogenesis effects in the chick chorioallantoic membrane (CAM) [69], chitosan-encapsulated loaded zinc ferrite for biocompatible drug delivery on chicken embryonic stem cells [70], and uncoated ferrite nanoparticles used in modulation of angiogenesis activity in Chick chorioallantoic membrane (CAM) [71]. In the (CAM) test, gold and silver nanoparticles conjugated with heparin derivative exhibit anti-angiogenesis characteristics [73]. Graphites, multiwalled carbon nanotubes, and fullerenes are examples of carbon compounds that block the growth factors that induce angiogenesis and vascular endothelial growth factor. [74].

Amine functionalized MFe_2O_4 (M = Co, Ni and Mn) promotes angiogenesis in (CAM) [75]. Gold and Silver NPs are found to be anti-angiogenesis properties in CAM, while iron oxide NPs are found to be angiogenenic properties in CAM [71, 73, 75]. There are not much reported data on iron oxide NPs as stimulate angiogenesis activity.

- **Angiogenesis activity in CAM:** To assess the impact of nanoparticles on angiogenesis, the Chick Chorioalantoic membrane model (CAM) was employed. White chick leg horn eggs, three days old, were bought from Central Poultry Organization in Goregaon, Mumbai. Following an ethanol cleaning, the eggs were incubated at 37 degrees Celsius. Using a tiny window in the eggshell, the test samples were injected into the eggs on the fifth day and covered with parafilm. Under 37°C, the eggs were incubated. The eggs were carefully cracked from the air sac location on the fourteenth day, and the embryo was separated to reveal the CAM. In each case, CAM was examined with a stereo microscope and captured on camera at a fixed distance using an 8 megapixel camera. Based on the number of blood vessels that split off from the main vessel and sprouted from the branched vessels, a score representing the degree of angiogenesis was assigned.

  Following isolation, CAM was homogenized for five minutes and diluted in fifteen milliliters of Drabkin's reagent to measure the hemoglobin content. A second centrifugation was performed on the CAM solution for 20 minutes at 1500 rpm. After separating the supernatant, measurements were made using a spectrophotometer at 570 nm. When potassium ferricyanide, potassium cyanide, and NaHCO3 are added to blood, haemoglobin combines with ferricyanide to generate met-haemoglobin, and then with cyanide to form cyan met-haemoglobin. This process is known as Drabkin's reagent. The product's color intensity, evaluated at 570 nm, is directly correlated with the hemoglobin concentration.

  The conversion of optical density into Hemoglobin level in terms of g/dL is carried out as follows: The hemoglobin level (g/dL) was determined by the following formula for 1ml of Drabkin's reagent:

$$\mathbf{Hb}\left(\frac{\mathbf{gms}}{\mathbf{dL}}\right) = \frac{\mathbf{O.D.\,of\,test}}{\mathbf{O.D.\,of\,standard}}\,\mathbf{X\,15.06}$$

O.D of test = Optical Density of test (iron oxide based NPs)
O.D of Standard = Optical Density of Standard hemoglobin

Eggs were treated in the study including 6 eggs (n=6) for each test concentration of the NPs.

Figure 4: Inoculation of drug through window on day 5.
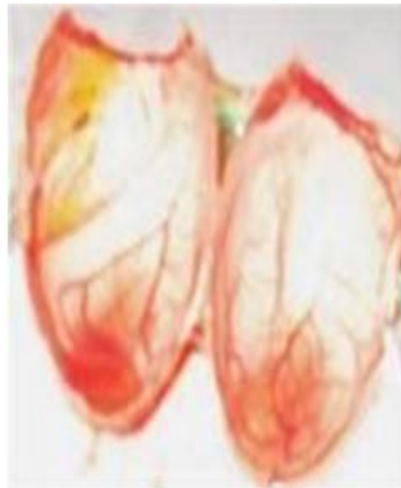
Figure 5: Isolation of CAM open on day 14.

Statistical analysis was carried out using standard methods for calculating mean, Standard Deviations (S.D.) and Student's t-test and ANOVA test etc.

In this study, we used Student's t-test because the sample size is small (N<100). The cell viability and angiogenesis activity in CAM model for finding the effect of synthesized NPs before and after adding the NPs. The test whether hypothesis is accepted or rejected in terms of p-value/t- value: these indicators are calculated from the standard statistical formulae.

The formula for finding the t value is:

$$t = \frac{X_{mean} - hypothesis\ value}{\frac{S_d}{\sqrt{n}}}$$

Where X_{mean} is mean of difference, hypothesis value = 0, S_d = Standard deviation and n = no. of population.

The t-value and p-values were calculated using Microsoft excel spreadsheets

V. MAGNETIC RESONANCE IMAGING (MRI) CONTRAST AGENTS

Nuclear magnetic resonance concepts have been used in the development of magnetic resonance imaging (MRI). This is an effective tool for creating a detailed virtualization of the inside structure of the body. It provides a way to see soft tissues and identify changes in an organism's physiology and chemistry. MRI is a diagnostic method based on interactions between a strong magnetic field and the protons in the human body. Since our bodies contain about 80% water, protons with unpaired spins on the hydrogen nucleus function very well as an instrument when exposed to an external magnetic field. Spins precess at a frequency known as precessional frequency, or Larmor frequency, along an axis of exposed magnetic field:

$\omega o = \gamma Bo$

In the context of this explanation, where ωo represents the recessional frequency, γ denotes the gyromagnetic ratio (which is the ratio of the magnetic moment to the angular momentum of a specific system, in our case, protons), and Bo stands for the magnetic flux density, magnetic resonance phenomena occur when a radiofrequency pulse is applied perpendicular to the magnetic field. During this process, protons absorb energy and transition from a stable initial state to an unstable excited state. Once the Larmor frequency pulse is removed, the excited spins reorient themselves to the equilibrium state parallel to Bo and release the absorbed energy in the form of radiation. This phenomenon is commonly referred to as spin relaxation. Since protons in different tissues possess distinct relaxation characteristics, variations in the signals are observed, which are then utilized to construct images of the anatomical features of the organism. Proton signals are recorded and processed through a mathematical algorithm to produce a visual representation. [76- 79]. The applications of NPs in medicine has led to the use of Superparamagnetic iron oxide nanoparticles (SPIONs) for therapeutic uses as magnetically guided drug delivery systems for treatment of cancer and for diagnostic purposes such as Magnetic Resonance Imaging (MRI) contrast agents [80]. The strength of MRI is its excellent discrimination between soft tissues, providing naturally the contrast between the structural differences of normal and pathological tissues. This visibility of internal body structures and contrast is further enhanced by the use of MRI contrast agents. The role of contrast agents in MRI is very important. There are two types of relaxation in MRI with times *T1* and *T2*, which occur simultaneously, independent of each other. The longitudinal *T1* relaxation time of water exhibit bright or positive contrast whereas transverse *T2* relaxation time of water produces dark or negative contrast. Relaxivitiy is a measure of the ability of MRI contrast agents to increase the relaxation of the surrounding nuclear spins (hydrogen protons), which can then be used to improve the contrast in MR imagesRelaxivity is quantified in units of mM-1s-1 for nanoparticles (NPs). The impact of paramagnetic contrast agents on the relaxation of nuclear spins arises from both inner and outer sphere processes. The inner sphere process results from the chemical interaction between the bonded water of paramagnetic agents and the surrounding free water molecules, leading to an increase in relaxation (with a more significant effect on T1) of nuclear spins. Conversely, the outer sphere process occurs when paramagnetic agents diffuse

through free water. During this process, the random movements of paramagnetic agents generate local magnetic field variations, consequently boosting the relaxation (with a greater impact on T2) of nuclear spins [81, 82].

In clinically utilized gadolinium-based contrast agents, gadolinium ions form chelates. Consequently, the bound water within these chelates maintains continuous interactions with the surrounding free water, augmenting the T2 relaxation of nuclear spins. Most gadolinium chelate agents exhibit a more pronounced inner sphere effect compared to the outer sphere effect, making them suitable as T1 contrast agents. In contrast, coated ferrite nanoparticle agents are completely enveloped by their coating material, preventing chemical interactions (inner sphere processes) from occurring. Additionally, ferrite nanoparticles possess a substantially greater magnetic moment than gadolinium ions, resulting in more significant magnetic field fluctuations (inhomogeneity). Due to these properties of magnetic nanoparticles, they are regarded as ideal T2 contrast agents. [82]. So contrast agents are classified as *T1* (positive) agents and *T2* (negative) agents. The process of imaging at high field (9 Tesla) and frequencies have been found to produce undesirable side effects in patients and techniques of imaging are developed to produce better resolution at moderate fields. This has been achieved by the use of suitable magnetic contrast agents with the ability to modulate the *T1* and *T2* relaxivities. These imaging techniques adopted *T1* and *T2* weighted sequences, depending on the tissues to be scanned. Currently, the conventional media used were paramagnetic gadolinium based agents are used for *T1*-weighted image that are relatively expensive and superparamagnetic iron oxide based magnetic NPs used for *T2*-weighted image [83- 87]. The conventional *T1* MRI contrast agents have heavy metals like Gd that are paramagnetic; there have been reports that these heavy elements leave traces in the brain over a long period of time. Hence there is a need to consider materials that are relatively safe and hence we have conducted a study on iron oxide based NP formulations which are relatively safe and non-toxic. The quality of MRI images depends upon the several parameters such as applied magnetic field, radio frequency, the proton spin density, the nuclear spinlattice relaxation time *T1*, the spin-spin relaxation time *T2*, contrast agents and nature of the tissues to be scanned [88-90]. *T1*-weighted scanning shows fat brighter but water darker and are called positive; *T2*-weighted scanning shows reverse – fat darker and water brighter, so called negative. *T1* sequence is more efficient for brain imaging, *T2* for spinal cord diagnostics [91].
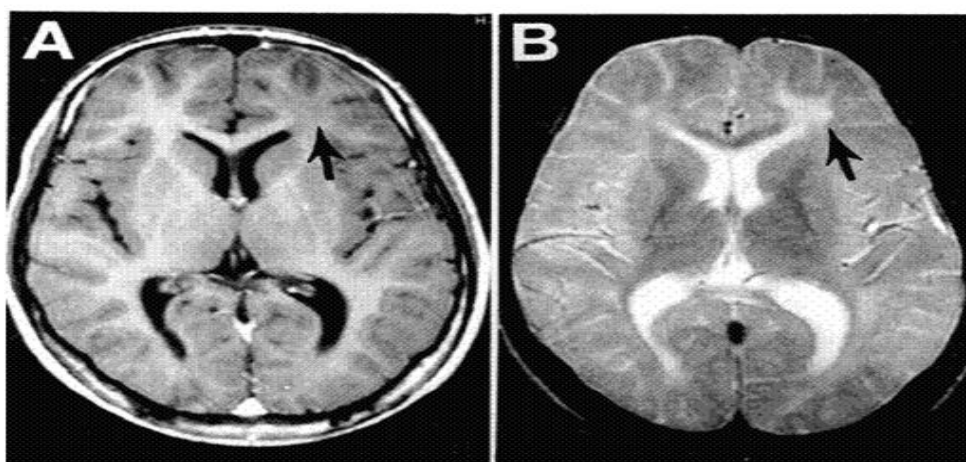
Figure 6: T1 (A) AND T2 (B) weighted images of human brain [89]

The SPIONs used as MRI T2 contrast agents must have combined properties of high magnetic saturation, size less than 50 nm, biocompatibility, pH neutrality, chemical stability and agglomeration free. The SPIONs used as MRI T2 contrast agents must have combined properties of high magnetic saturation, size less than 50 nm, biocompatibility, pH neutral, chemical stability and agglomeration free. The main problem with SPIONs is their fast agglomeration in water due to the high surface to volume ratio and magnetization. To reduce agglomeration these NPs are coated with various polymers such as dextran, chitosan, polyethylene glycol (PEG), polyvinyl alcohol (PVA) etc. to enhance biocompatibility, and longer shelf life and are successfully used as MRI contrast agents [92-95]. Numerous pieces of literature have documented the utilization of superparamagnetic iron oxide nanoparticles (SPIONs) as MRI T2 contrast agents. These include the use of uniform mesoporous silica coated with iron oxide NPs for MRI T2 contrast agents [96], chitosan-coated SPIONs employed as MRI contrast agents in vivo [97], folic acid-conjugated glucose and dextran-coated iron oxide NPs for MRI contrast [98], polyvinyl pyrrolidone (PVP) functionalized SPIONs for MRI contrast [99], amine-functionalized iron oxide NPs for T2 contrast agents [100], and Manganese ferrite NPs conjugated with gadolinium and folic acid to achieve dual contrast T1 and T2-weighted MR images in hela cells [101]. Hence, the key challenge in this field lies in the development of high-quality aqueous iron oxide NPs that are biocompatible and capable of delivering enhanced relaxation effects compared to the currently available commercial MRI contrast agents [102].

In the present thesis, we have synthesized a series of such Ferrite NPs both uncoated and coated with different organic, inorganic and polymer materials, by various chemical synthetic procedures. They have been characterized by various complementary techniques that are briefly discussed. The test for biocompatibility has been carried out in vitro on cell lines of human lymphocytes. The applicability of these formulations as *T2* MRI contrast agents was examined on a clinical MRI machine. The effect of the NP formulations into the chick chorioallantoic membrane (CAM) of fertile leghorn chick eggs was examined in-vitro for studying the bioactivity of angiogenesis that deals with the formation of new blood vessels from pre-existing vessels.

1. **Scope of study:** Numerous possible uses for magnetic nanoparticles (NPs), from ultra-high density information storage to biological applications, as well as soft to hard magnetic materials, have sparked interest in research recently. Since contrast agents are used in magnetic resonance imaging (MRI), numerous efforts have been undertaken to increase their relaxivity. Several Iron oxide based NPs and related formulations are identified as *T2* MRI contrast agents. Iron oxide based NPs have to meet several specifications in order to be applied *T2* MRI contrast agents. Important features of these NPs are that they should have are a small overall size, superparamagnetism, high colloidal stability in water, (ie the NPs suspension in water does not settle down when large field is applied) and biocompatibility both for *in vitro* and *in vivo* applications. Comparative studies of synthesis and characterization of iron oxide based NPs are carried out. The cytotoxicity of the synthesized NPs with lymphocytes and their use as *T2* contrast agents in MRI was investigated.

2. **MRI measurement:** The *T2* relaxation times (sec) measurement was done using a 3T clinical MR Scanner (General Electric Healthcare, USA). Samples of different concentrations of magnetic NPs were prepared by diluting them with distilled water for

aqueous solutions and Minimum Essential Medium (MEM) for cells. $T2$ weighted images were obtained with a multiple fast spin echo pulse (FSE) sequence (repetition time TR = 3500 ms; echo time TE = 15, 30, 45, 60, 75 and 90 ms; matrix 512 x 512). For MRI analysis the aqueous solution of magnetic NPs are taken in Elisa plate i.e. (0.2, 0.1. 0.08, 0.04, 0.02, 0.01, 0.005 and 0 mM) and treated with human lymphocyte cells i.e. (0.4, 0.2, 0.16, 0.08, 0.04, 0.02, 0.01 and 0 mM) at eight different Fe concentrations. The Fe concentration used for NPs treated with lymphocyte cells are twice to those of aqueous solutions (untreated with cells). The image obtained from MRI machine is in Dicom file and is converted into jpeg or tiff format by RadiAnt Dicom viewer software. The $T2$ value is calculated by ImageJ MRI plugin calculator. The $r2$ ($1/T2$) relaxivity values in (mM-1 s-1) were calculated from the slope of the linear plots of $1/T2$ versus the Fe concentrations and the formula is given below:

$$\frac{1}{T_2} = \frac{1}{T_2^o} + r_2[Fe]$$

The observed relaxation rate in the presence of iron oxide nanoparticles is represented by $1/T_2$. The transverse relaxation rate is r_2 ($1/T_2$), the concentration of Fe ions is [Fe], and the relaxation rate of pure water is $1/T^o_2$ [103].

VI. CONCLUSIONS

The present study was aimed at discuss in detail methods commonly used in synthesis of magnetic nanoparticles (NPs) with various coatings and characterization with XRD, Raman spectroscopy, FTIR, UV-Visible Spectroscopy, BET, DLS, magnetization and SEM. The next step was to evaluate biocompatibility of NPs with human lymphocyte cells and study their effect of angiogenesis activity in CAM model. The intended application as MRI contrast agents of the NPs in aqueous has been studied in deep. The descriptive method for MRI to carry out on the lymphocyte cells incubated with NPs has been studied. In future scope, it is possible to design and develop applications based on these multifunctional properties eg. optofluidic, magneto-optic,magneto-fluidic sensors and probes that can act as diagnostic and therapeutic probes, and is also theranostic applications.

REFERENCES

[1]   Q. A. Pankhurst, J. Conolly, S. K. Jones and J Dobson, J. Phys. D: Appl. Phys. 36 (2003) R167-R181, doi: 10.1088/0022-3727/36/13/201
[2]   Y. Li, W. Kim, Y. Zhang, M. Rolandi, D Wang and H. Dai, J. Phys. Chem. B, 105 (2001) 11424-11431, doi: 10.1021/jp012085b
[3]   H W. Zhang, Y. Lui, S H. Sun, J. Frontiers of Phys in China. 5 (2010) 347-356, doi: 10.1007/s11467-010-0104-9
[4]   J R. Stephens, J S. Beveridge and M E. Williams, Phys. Chem. Chem. Phys. 14 (2012) 3280- 3289, doi: 10.1039/c2cp22982j
[5]   R. Y. Hong, T. T. Pan, Y. P. Han, H. Z. Li, J. Ding, H. Sijin, J. Magn. Magn. Mater. 310
[6]   (2007) 37-47, doi: 10.1016/j.jmmm.2006.07.026
[7]   A. S. Arbab, L. A. Bashaw, B. R. Miller, E. K. Jordan, B. K. Lewis, H. Kalish, H. J. A. Frank, Radiology. 229 (2003) 838-846, DOI: http://dx.doi.org/10.1148/radiol.2293021215
[8]   C. Sun, C. Fang, Z. Stephen, O. Veiseh, S. Hansen, D. Lee, R. G. Ellenbogen, J. Olson, M. Zhang, Nanomedicine (Lond). 3 (2008) 495-505, doi: 10.2217/17435889.3.4.495
[9]   R. Y. Hong, B. Feng, L. L. Chen, G. H. Liu, H. Z. Li, Y. Zhang and D. G. We, Biochem. Eng. J. 42 (2008) 290-300, doi: 10.1016/j.bej.2008.07.009

[10] G. Y. Li, Y. Jiang, K. Huang, P. Ding and P. Chen, J. Alloys. Comp. 466 (2008) 451-456, doi: 10.1016/j.jallcom.2007.11.100

[11] A. B. Salunkhe, V. M. Khot, N. D. Thoral, M. R. Phadatare, C. I. Sathish, D. S. Dhawale and S. H. Pawar, App. Surface. Sci. 264 (2013) 598-604, doi: 10.1016/j.apsusc.2012.10.073

[12] A. Mukhopadhyay, N. Joshi, K. D. Chattopadhyay and G. A. Facile, App. Mater. Interfaces.

[13] 4 (2012) 142-149, http://dx.doi.org/10.1021/am201166m

[14] R de Lima, JL de Oliveira, A. Ludescher, MM. Molina, R. Itri, AB. Seabra and PS. Haddad, Journal of Phys: Conference Series. 429 (2013) 1-7, doi:10.1088/1742-6596/429/1/012034

[15] S. F. Shi, J. F. Jia, X. K. Guo, Y. P. Zhao, D. S. Chen, Y. Y. Gou, T. Cheng, X. Y. Zheng, Int. J. NanoMedicine. 7 (2012) 5593-5602, doi: 10.2147/IJN.S34348

[16] J. Sun, S. Zhou, P. Hou, Y. Yang, J. Weng, X. Li, M. Li. J. Biomed. Material Research Part A. 80A (2007) 333-341, doi: 10.1002/jbm.a.30909

[17] C. M. Hurd, "Varieties of magnetic order in solids", CONTEMP. PHYS. 23 (1982) 469-493,

[18] http://dx.doi.org/1010.1080/00107518208237096

[19] C. D. Stanciu, A. V. Kimel, F. Hansteen, A. Tsukamoto, A. Itoh, A. Kirilyuk and Th. Rasing, Phys. Rev. B, 73 (2006) 220402(R), doi: 10.1103/PhysRevB.73.220402

[20] B. D. Cullity, Introduction to Magnetic Materials, Addison -Wesley, MA (1972) 18] J. Frenkel, J. Doefman: Nature, 126 (1930) 274-275, doi: 10.1038/126274a0

[21] C. P. Bean, J. D. Livingston, J. Appl. Phys, Supplement to 30 (4) (1959) 120S-129S,

[22] http://dx.doi.org/10.1063/1.2185850

[23] L. Neel, Ann. Geophys. 5 (1949) 99-136.

[24] L. Neel, CR Acad. Sci. 252 (1961) 4075-4080

[25] L. Neel (Eures Scientifiques (1978) Editions du CNRS Paris English translation:

[26] Selected works of Louis Neel (1988) Gordon & Breach, Sci - Publishers, New York, London. 23] P. Patnaik, Dean's Analytical Chemistry Handbook, 2nd ed. McGraw-Hill, 2004.

[27] D. Harvey, Modern Analytical Chemistry, McGraw-Hill (2000). ISBN: 10 0-7141060-0 25] A. H. Li, E. L. Salabas and F. Schuth, Angrew. Chem., Int. Ed., 46 (2007) 1222-1244, doi: 10.1002/anie.200602866

[28] G. Gnanaprakash, S. Ayyappan, T. Jayakumar, John Philip and Baldev Raj, Nanotechnology,

[29] 17 (2006) 17: 5851-5857, doi:10.1088/0957-4484/17/23/023

[30] G. Gnanaprakash, John Philip, T. Jayakumar and Baldev Raj J. Phys. Chem. B, 111 (2007) 7978-7986, doi: 10.1021/jp071299b

[31] S. Ayyappan, John Philip and Baldev Raj, J. Phys. Chem. C, 113 (2009) 590-596, doi: 10.1021/jp8083875

[32] S. Ayyappan, S. Mahadevan, P. Chandramohan, M. P. Srinivasan, John & Philip and Baldev Raj, J. Phys. Chem. C, 114 (2010) 6334-6341, doi: 10.1021/jp9.11966p

[33] M. A. Willard, L. K. Carpenter, E. E. Calvin, S. Calvin, V. G. Harris, Int. Mater. Rev. 49

[34] (2004) 125-170, doi: 10.1179/095066004225021882

[35] I. J. Bruce, J. Taylor, M. Todd, M. J. Davies, E. Borioni, C. Sangregorio, T. Sen, J. Magn. Magn. Mater. 284 (2004) 145-160, doi: 10.1016/j.jmmm.2004.06.051

[36] S. Khalafalla, G. Riemers, IEEE Trans. Magn. 16 (2) (1980) 178-183, doi: 10.1109/TMAG.1980.1060578

[37] L. Babes, B. Denizot, G. Tanguy, J. J. Le Jeune, P. Jallet, J. Colloid Interface. 212 (1999) 474-482.

[38] J. Park, K. An, Y. Hwang, J-G. Park, H-J. Noh, J-Y. Kim, J-H Park, N-M. Hwang, T. Hyeon, Nat. Mater. 3 (2004) 891-895., doi: 10.1038/nmat1251

[39] P. Tartaj, M. P. Morales, S. Veintemillas-Verdaguer, T. Gonzalez-Carreno, C. J. Serna, Handbook of Magnetic Materials, 9 (2006) 403-533, doi: 10.1016/S1567-2719(05) 16005-3

[40] Y. Li, M. Afzaal, P. O'Brien, J. Mater. Chem. 16 (2006) 2175-2180, doi: 10.1039/B517351E

[41] A. Domortiere, P. Panissod, B. P. Pichon, G. Pourroy, D. Guillon, B. Donnio, S. Begin-Colin, Nanoscale, 3 (2011) 225-232, doi: 10.1039/c0nr00521e

[42] S. F. Chin, S. C. Pang, C. H. Tan., J. Mater. Environ. Sci. 2 (2011) 329-302, ISSN: 2028-

[43] 2508

[44] S. L. Peshkovsky, and A. S. Peshkovsky, , Ultrason. Sonochem., 14 (2007)   314–322,

[45] doi:10.1016/j.ultsonch.200607.003

[46] A.S. Peshkovsky and S.L. Peshkovsky, Sonochemistry: Theory, Reactions and Syntheses, and Applications, Hauppauge, NY: Nova Science Publishers (2010)

[47] A.S. Peshkovsky and S.L. Peshkovsky, Book Series: Physics Research and Technology, Hauppauge, NY: Nova Science Publishers (2010)

[48] K. S. Suslick, "Sonochemistry", Science 247 (1990) 1439-1990, doi: 10.1126/science247.4949.1439.

[49] K. S. Suslick and D. J. Flannigan, Annual Rev. Phys. Chem. 59 (2008) 659-683, doi:

10.1146/annurev.physchem.59.032607.093739

[50] K. S. Suslick and S. Kenneth , The Chemical Effects of Ultrasound, Scientific American, (1989) 62-68.

[51] N. Lewinski, V. Colvin, and R. Drezek "Cytotoxicity of Nanoparticles" Wiley-VCH Verlag GmbH&Co. KGaA, Weinheim , Small, 4 (2008) 26 -49 doi: 10.1002/smll.200700595

[52] Zhao, X., Hilliard, L. R., Wang, K., and Tan, W. (2004) Bioconjugated silica nanoparticles for bioanalysis. In Encyclopedia of Nanoscience and Nanotechnology (Nalwa, H. S., Ed.) pp 255– 268, American Scientific Publishers, Stevenson Ranch. 4

[53] Kairemo Kalveli, Paola Erba, Kim Bergstrom and Ernest K.J. Pauwels; "Nanoparticles in cancer", 1 (2008) 30-36.

[54] J. Wang, P. F. Chong, S. C. Ng, L. M. Gan, Mater. Lett. 30 (1997) 217-221, doi: 10.1016/S0167-577X(96)00200-5

[55] T. Brunner, P. Wick, P. Manser, P. Spohn, R. Grass, L. Limbach, A. Bruinink, W. Stark, Environ. Sci. Technol. 40 (2006) 4374 – 4381.

[56] F. Y. Cheng, C. H. Su, Y. S. Yang, C. S. Yeh, C. Y. Tsai, C. L. Wu, M. T. Wu, D. B. Shieh,

[57] Biomaterials, 26 (2005) 729–38,doi: 10.1016/j.biomoterials.2004.03.016

[58] S. M. Hussain, K. L. Hess, J. M. Gearhart, K. T. Geiss, J. J. Schlager, Toxicol. In Vitro, 19

[59] (2005) 975–983, doi: 10.1016/j.tiv.2005.06.034

[60] A. K. Gupta, S. Wells, IEEE Trans. Nanobiosci. 3 (2004) 66–73.

[61] S. Wan, J. Huang, M. Guo, H. Zhang, Y. Cao, H. Yan, K. Liu, J. Biomed. Mat. Res. Part A.

[62] 80A (2007)946–954, doi: 10.1002/jbm.a.31022

[63] Hafeli U.O, Gayle J. Pauer, "In vitro and in vivo toxicity of magnetic microspheres", Journal of Magnetism and Magnetic Materials, 194 (1999) 76-82

[64] Nooris Momin, Aparna Deshmukh and Radha S, J. Nanoresearch, 34 (2015) 1-8, doi: 10.4028/www.scientific.net/JNanoR.34.1

[65] W. Risau and I. Flamme, "Vasculogenesis". Annual review cell and development biology, 11

[66] (1995) 73-91, doi: 10.1146/annurev.cb.11.110195.000445

[67] D. Hanahan and J. Folkman, Cell. 86 (1996)353-364, doi: 10.1016/S0092-8674(00)80108-7

[68] P. Carmeliet and R. K. Jain, Nature. 407 (2000) 249-257, doi:10.1038/35025220

[69] J. Wilting, H. Neeff and B. Christ. Cell Tissue Res., 297 (1999) 1-11.

[70] P. Osbody, M. J. Oursler, T. Salino-Hugg and M. Krukowski, Ciba Found. Symp, 136 (1988) 108-124.

[71] D. Rabitta, Int. Rev. Cell. Mol. Biol, 270 (2008) 181-224.

[72] A. M. Cimpean, D. Ribatti, M. Raica, Angiogenesis, 11 (2008) 311-319, doi: 10.1007/s10456- 008-91171

[73] P. R. Woolcock, Methods Mol. Biol. 436 (2008) 35-46, doi: 10.1007/978-1-59745-279-3_6

[74] J. S. Guy, Methods Mol. Biol. 454 (2008) 109-117.

[75] B. Fried and L. T. Stablefor, Adv. Parasitol. 30 (1991) 108-165.

[76] D. Rabitti, Methods Mol. Biol, 843 (2012) 47-57, doi: 10.1007/978-1-61779-523-7_5

[77] R. W. Cole, F. Liu and B. J. Herron, Microscopy: Science, Technology, Applications and Education, (2010) 885-896.

[78] G. Sun, X. Zhang, Y. Shen, R. Sebastain, L. E. Dickinson, K. F. Talbot, M. Reinblatt, C. Steenbergen, J. W. Harmon and S. Gerecht, Prooceedings of the National Academy of Sciences of the United States of America 108 (2011) 20976-20981, doi: 10.1073/pnas.1115973108

[79] L. Guedez, A. M. Rivera, R. Salloum, M. L. Miller, J. J. Diegmueller, P. M. Bungay and W.

[80] G. Stetler-Stevenson , American Journal of Pathology, 162 (2003) 1431-1439, doi: 10.1016/S0002-9440(10)64276-9

[81] V. J. Sawant, S. R. Bamane and S. M. Pachchapurkar, Der Chemica Sinica, 4 (2013) 67-78.

[82] ISSN: 0976-8505

[83] Aparna Deshmukh, S. Radha, Y. Khan and Priya Tilak, AIP Conf. Proc. 1349 (2011) 437-438,

[84] doi: 10.1063/1.3605922

[85] J. Baharara, F. Namvar, M. Mousavi, T. Ramezani and R. Mohamad, Molecules, 19 (2014) 13498-13508. doi: 10.3390/molecules190913498

[86] M. M. Kemp, A. Kumar, S. Mousa, E. Dyskin, M. Yalcin, P. Ajayan, R. J. Linhardt and S. A. Mousa, Nanotechnology 20 (2009) 1-7, doi: 10.1088/0957-4484/20/45/455104

[87] S. Murugesan, S. A. Mousa, L.J. Connor, D. W. Lincoln and R. J. Linhardt, FEBS Letters. 581

[88] (2007) 1157-1160. doi: 10.1016/j.febslet.2007.02.022

[89] Nooris Momin, Aparna Deshmukh and Radha S, European BioPhys. J. (2015) 1-10, doi:

[90] 10.1007/s00249-015-1083-0

[91] R. H. Hashemi, W. G. Bradley, C. J. Lisanti, J. Magn. Reso. Imag. 7 (1997) 614-615. 77] M. P. Hiorns,

Pediatr Nephrol, 26 (2011) 59-68, doi: 10.1007/s00467-010-1645-4

[92] D. Formica and S. Silvestri, Bio. Med. Eng. 3 (2004) 1-12, doi: 10.1186/1475-925X-3-11 79] J. P. Ridgway, Journal of Cardiovascular Magnetic Resonance, 12 (2010) 7-15, doi: 10.1186/1532-429X-12-71

[93] C. Sun, C. Fang, Z. Stephen, O. Veiseh, S. Hansen, D. Lee, R. G. Ellenbogen, J. Olson and M. Zhang, Nanomedicine (Lond)., 3 (2008) 495-505, doi: 10.2217/17435889.3.4.495

[94] T. Ahmad, H. Bae, Y. Iqbal, I. Rhee, S. Hong, Y. Chang, J. Lee, D. Sohn, J. Magn. Magn. Mater. 381 (2015) 151-157, doi: 10.1016/j.jmmm.201412.077

[95] R. B. Lauffer, Chem. Rev. 87 (1987) 901-927, doi: 10.1021/cr00081a003

[96] P. Caravan, J. J. Ellison, T. J Mc Murry, and R. B. Lauffer, Chem. Rev., 99 (1999) 2293-2352,

[97] doi: 10.1021/cr980440x

[98] C. Wilhelm, F. Gazeau, Biomaterials, 29 (2008), 3161-3174,doi: 10.1016/j.biomaterials.2008.04.016

[99] B. Chertok, B. A. Moffat, A. E. david, F. Yu, Bergemann C, B. D. Ross, V. C. Yang, Biomaterials., 29 (2008) 487-496, doi: 10.1016/j.biomaterials2007.08.050

[100] N. Nasongkla, E. Bey, J. Ren, H. Ai, C. Khemtong, J. S. Guthi, S. F. Chin, A. D. Sherry, D. A. Boothman, J. Gao. Nano Lett., 6 (2006) 2427-2430, doi: 10.1021/nl061412u

[101] J. Wang, B. L. Zhang, G. yang, L. Wang, S. B. Xie, L. Xuan, F. B. Gao, Journal of inorganic materials., 30 (2015) 53-58, doi: 10.15541/jim20140178

[102] M. G. Landsberg, M. Straka, S. Kemp et al., Lancet Neurology., 11 (2012) 860-867, doi: 10.1016/S1474-4422(12)70203-X

[103] D. E. Sosnovik, M. Nahrendorf and R. Weissleder, Circulation, 115 (2007) 2076-2086, doi: 10.1161/CIRCULATIONAHA,.106.658930

[104] P. V. Prasad, AJP Renal Physiology, 290 (2006) F958-F974, doi: 10.1152/ajprenal.001142005 91] W. P. Dillon, Neuroimaging in Neurologic Disorders, Harrison's Principles of Internal Medicine, 17th Edi. (2008) 2491-2497. ISSN-13: 978-0071466332

[105] H. T. Chan, Y. Y. Do, P.L. Huang, P.L. Chien, T. S. Chan, R.S. Liu, C. Y. Huang, S. Y. Yang,

[106] H.E. Horny. J. Magn. Magn. Mater., 304 (2006) 415-417.

[107] M. Yu, S. Huang, K. J. Yu and A. M. Clyne. Int. J. Mol. Sci., 13 (2012) 5554-5570.

[108] M. Mahdavi, M. B. Ahmad, M. J. Haron, F. Namvar, B. Nadi, M. Z. Ab Rahman and J. Amin. Molecules., 18 (2013) 7533-7548, doi: 10.3390/molecules18077533

[109] S. F. Shi, J. F. Jia, X. K. Guo, Y. P. Zhao, D. S. Chen, Y. Y. Guo, T. Cheng and X. L. Zhang. Int. J. Nanomedicine., 7 (2012) 5593-5602, doi: 10.2147/IJN.S34348

[110] F. Ye, S. Laurent, A. Fornara, L. Astolfi, J. qin, A. Roch, Alssandro Martini, S. M. Toprak, R.

[111] N. Muller and M. Muhammed. Contrast Media Mol. Imaging, 7 (2012) 460-468, doi: 10.1002/cmmi1473

[112] A. M. Reddy, B. K. Kwak, H. J. Shim, C. Ahn, H. S. Lee, Y. J. Suh and E. S. Park. J. Korean Med Sci., 25 (2010) 211-219, DOI: http://dx.doi.org/10.3346/jkms.2010.25.2.211

[113] F. Dai, M. Du, Y. Liu, G. Liu, Q. Liu and X. Zhang, J. Mater. Chem. B., 2 (2014) 2240-2247,

[114] doi: 10.1039/c3tb21732a

[115] Arsalani H. Fattahi and M. Nazarpoor, eXPRESS Polymer Letters., 4 (2010) 329-338. 100] K. C. Barick, M. Aslam, Y. P. Lin, D. Bahadur, P. V. Prasad, P. Vinayak and P. Dravid. J. Mater. Chem., 19 (2009) 7023-7029, doi: 10.1039/b911626e

[116] Z. Wang, J. Liu, T. Li, J. Liu and B. Wang. J. Mater. Chem. B., 2 (2014) 4748-4753, doi: 10.1039/C4TB00342J

[117] F. Q. Hu, L. Wei, Z. Zhou, V. L. Ran, Z. Li and M. Y. Gao, Adv. Mater., 18 (2006) 2553-

[118] 2556, doi: 10.1002/adma.200600385

[119] J. Wan, W. Cai, X. Meng and E. Liu, Chem. Commun., (2007), 5004-5006, doi: 10.1039/b712795b